HHS Public Access

Author manuscript

Nat Med. Author manuscript; available in PMC 2015 March 01.

Published in final edited form as:

Nat Med. 2014 September ; 20(9): 1009–1017. doi:10.1038/nm.3586.

Non-canonical Wnt4 prevents skeletal aging and inflammation by inhibiting NF-κB

Bo Yu[1,7], **Jia Chang**[1,7], **Yunsong Liu**[2], **Jiong Li**[1], **Kareena Kevork**[1], **Khalid Al-Hezaimi**[3], **Dana T Graves**[4], **No-Hee Park**[5], and **Cun-Yu Wang**[1,6,*]

[1]Laboratory of Molecular Signaling, Division of Oral Biology and Medicine, School of Dentistry and Broad Stem Cell Research Center, UCLA, Los Angeles, CA 90095, USA

[2]Department of Prosthodontics, School and Hospital of Stomatology, Peking University, Beijing 100081, China

[3]Eng.A.B Research Center for Growth Factors and Bone Regeneration, Division of Periodontology, College of Dentistry, King Saud University, Riyadh 11545, Saudi Arabia

[4]Department of Periodontics, School of Dental Medicine, University of Pennsylvania, Philadelphia, PA 19104, USA

[5]School of Dentistry and Jonsson Comprehensive Cancer Center and David Geffen School of Medicine, UCLA, Los Angeles, CA 90095, USA

[6]Department of Bioengineering, Henry Samueli School of Engineering and Applied Science, UCLA, Los Angeles, CA 90095, USA

Abstract

Aging-related bone loss and osteoporosis affect millions of patients worldwide. Chronic inflammation associated with aging and arthritis promotes bone resorption and impairs bone formation. Here we show that Wnt4 attenuated bone loss in osteoporosis and skeletal aging by inhibiting nuclear factor-kappa B (NF-κB) via non-canonical Wnt signaling. Transgenic mice expressing Wnt4 from osteoblasts were significantly protected from bone loss and chronic inflammation induced by ovariectomy, tumor necrosis factor or natural aging. In addition to promoting bone formation, Wnt4 could inhibit osteoclast formation and bone resorption. Mechanistically, Wnt4 inhibited transforming growth factor beta-activated kinase 1-mediated NF-κB activation in macrophages and osteoclast precursors independent of β-catenin. Moreover, recombinant Wnt4 proteins were able to alleviate osteoporotic bone loss and inflammation by

*To whom correspondence should be addressed to C.Y.W (cunywang@ucla.edu).

[7]These authors contributed equally to this work

AUTHOR CONTRIBUTIONS

B.Y., J. C., Y.L., J.L., and K.K. performed the experiments. K.A-H., D.T.G., N.H.P. and C.Y.W designed experiments and analyzed data. B.Y. and C.Y.W. wrote the manuscript.

COMPETING INTERESTS STATEMENT

The authors declare that they have no competing financial interests.

inhibiting NF-κB *in vivo*. Taken together, our results suggest that Wnt4 might be used as a therapeutic agent for treating osteoporosis by attenuating NF-κB.

Normal bone remodeling maintains constant bone mass by an orchestrated balance between the destruction of pre-existing bone by osteoclasts and rebuilding by osteoblasts[1,2]. Aging brings significant changes to the skeletal system, characterized by structural alterations including reduction in trabecular bone volume, density and strength[3,4], as well as a shift in tissue microenvironment with increasing pro-inflammatory cytokine levels in bone marrow and the serum[5–8]. Advancing age is also a critical risk factor for osteoporosis which is the most common metabolic bone disease and a leading cause of morbidity and mortality in our aging population[9–11]. In osteoporosis, bone homeostasis is dysregulated by hormonal deficiency and aging, leading to increased bone turnover with enhanced bone formation and even greater rates of bone resorption, resulting in a net bone loss. Skeletal aging also manifests through other scenarios of abnormal bone remodeling, such as reduced formation and accelerated resorption in inflammatory bone diseases, and low bone turnover in physiological aging. Both arms of bone remodeling are regulated on the local level by factors secreted by bone cells, as well as on the systemic level by hormones[4,11–14].

Chronic inflammation has been found to be associated with osteoporosis and aging-related bone loss[1,6,7]. In general, the transcription factor NF-κB is activated during inflammatory processes[15]. Growing evidence suggests that NF-κB plays an important role in age-related disorders, including age-related bone loss and osteoporosis[16–19]. Inhibition of NF-κB has been shown to attenuate osteoporosis or arthritis[20,21]. We previously reported that NF-κB activation inhibits bone formation in estrogen deficiency-induced osteoporosis[22]. Thus, targeting NF-κB may allow both inhibition of bone resorption as well as promotion of bone formation. The Wnt family proteins are key regulators in growth and development, stem cell self-renewal, and cancer development[23,24]. Wnt signaling has also emerged as a critical player in bone homeostasis[25,26]. The 19 Wnt family proteins are divided into canonical and non-canonical ligands based on their dependence on transduction through β-catenin[27–29]. While there have been a few studies elucidating the role of non-canonical Wnt in osteoblast differentiation[30–33], little is known regarding how non-canonical Wnt affects osteoclast formation. Wnt5a-Ror2 signaling is found to promote osteoclastogenesis by activating the Wnt-c-Jun terminal kinase (JNK) pathway[32]. Previously, we found that Wnt4, a prototypical non-canonical Wnt ligand, is able to promote osteoblast differentiation of mesenchymal stem cells (MSCs)[33]. To further explore the therapeutic potential of Wnt4, we generated transgenic mice (Wnt4 mice) that express Wnt4 in osteoblasts. While we confirmed that Wnt4 could enhance bone formation *in vivo*, we found that Wnt4 could inhibit osteoclast formation and inflammation *in vivo*, thus attenuating bone loss and osteoporosis.

RESULTS

Wnt4 promotes bone formation *in vivo*

To explore whether Wnt4 promoted bone formation *in vivo*, we generated transgenic mice in which Wnt4 was driven by the mouse 2.3 kb type 1 collagen (Col2.3) promoter. The Col2.3 promoter contains a 2.3 kb DNA fragment upstream of the transcription start site of the

Col1a1 gene[34], and has been shown to drive gene expression specifically in differentiated osteoblasts[35]. After zygote injection, seven of the ten potential founders screened displayed strong expression of the transgene (Supplementary Fig. 1a), thus allowing establishment of two separate transgenic mouse lines (TG1 and TG7). While transgenic Wnt4 proteins were undetectable in primary calvarial cells from WT mice, Wnt4 proteins in calvarial cells from TG1 and TG7 mouse lines were induced as the cells differentiated into osteoblasts in osteogenic media (Fig. 1a). Reverse transcriptase-polymerase chain reaction (RT-PCR) confirmed that Wnt4 transgene mRNA was expressed in bone tissue, but not in brain, heart, kidney, liver, spleen, or muscle using the TG7 line (Fig. 1b). Next we investigated if Wnt4 would enhance bone formation *in vivo* using the TG7 line. Of note, Wnt4 mice had a phenotypically normal skeleton at birth (data not shown). μCT analysis of the secondary spongiosa of distal femur metaphysis revealed that the bone mineral density (BMD) of Wnt4 mice was significantly higher compared to wild-type littermates (WT) at 1, 2 and 3 months (Fig. 1c,d). Similarly, bone volume/tissue volume (BV/TV) was significantly higher in Wnt4 mice compared to WT mice (Fig. 1e), in consistence with the greater amount of trabecular bones shown in HE staining (Fig. 1f). Histomorphometric analysis revealed mildly higher osteoblast counts in 3-month-old Wnt4 mice compared to WT mice (Fig. 1g). To further confirm the increased BMD was due to enhanced osteoblast function, we performed dynamic histomorphometric analysis over a 7-day period using calcein labeling[22], and found that bone formation rate (BFR) in 3-month-old Wnt4 mice was significantly higher compared to WT mice (Fig. 1h). Similarly, characterization of the TG1 mouse line also confirmed that Wnt4 enhanced bone formation *in vivo*, ruling out variations due to mouse strains (Supplementary Fig. 1b,c).

To examine if Wnt4 enhanced osteoblastic activity in a cell-autonomous manner, we isolated bone marrow MSCs from femurs of Wnt4 mice and WT mice. Primary MSCs from Wnt4 mice demonstrated enhanced osteogenic potential, as evidenced by alkaline phosphatase (ALP) staining and Alizarin Red staining (ARS), when cells were induced by osteogenic medium (Fig. 1i,j). Furthermore, Real-time RT-PCR showed greater mRNA expression of the master osteogenic transcription factors *Runx2* and *Sp7* (Supplementary Fig. 1d,e), as well as mineralization markers *Ibsp* and *Biglap* (Supplementary Fig. 1f,g) in differentiated osteoblasts from Wnt4 mice compared with WT mice.

Wnt4 prevents estrogen deficiency-induced osteoporosis

To mimic the molecular pathogenesis of osteoporotic bone loss, mouse ovariectomy (OVX) has been widely used as a model to induce estrogen deficiency-mediated osteoporosis[6,22,36]. We performed OVX or sham operation on 3-month-old WT and Wnt4 mice. μCT analysis of femurs revealed significant trabecular bone loss in WT mice compared to sham control 2 months post OVX. In contrast, bone loss was markedly lower in Wnt4 mice after OVX (Fig. 2a). Quantitative measurements showed that, whereas 47% of BMD and 48% of BV/TV were lost in WT mice after OVX, only 27% of BMD and 24% of BV/TV were lost in Wnt4 mice (Fig. 2b). Following OVX, BFR increased in WT mice to compensate for the accelerated bone resorption, while in Wnt4 mice, osteoblastic activity was further enhanced (Fig. 2c). Similarly, osteoblast number and surface were significantly higher in Wnt4 versus WT mice in both OVX and sham groups (Fig. 2d). In contrast, we observed lower osteoclast

number and surface in Wnt4 mice compared to WT mice in both OVX and sham groups (Fig. 2e,f). We also performed ELISA to assess the serum markers of bone turnover. The serum concentrations of osteocalcin (Ocn), a marker for bone formation, were significantly higher in Wnt4 mice compared to WT mice after OVX (Fig. 2g). In contrast, OVX induced higher serum concentrations of Trap5b, a marker for bone resorption[37], in WT but not in Wnt4 mice (Fig. 2h).

Studies have implicated pro-inflammatory cytokines, including tumor necrosis factor (Tnf) and interleukin-6 (Il-6), as important mediators of accelerated bone loss in osteoporosis[38,39]. Consistently, OVX induced an elevation in serum concentrations of Tnf and Il-6 in WT mice, but such induction was suppressed in Wnt4 mice (Fig. 2i). Immunostaining of activated p65 in femur sections revealed enhanced NF-κB activity in osteoclasts and bone marrow cells surrounding trabecular bones following OVX. In contrast, the NF-κB activation by OVX was significantly less pronounced in Wnt4 mice (Fig. 2j). To further confirm the inhibition of NF-κB by Wnt4 *in vivo*, we immunostained NF-κB-dependent targets, including Tnf, Cycloxygenase-2 (Cox-2) and Matrix metallopeptidase 9 (Mmp9). Consistently, we found that Wnt4 also potently reduced the expression of Tnf, Cox-2 and Mmp9 induced by OVX *in vivo* (Supplementary Fig. 2a–c).

Wnt4 inhibits inflammatory bone loss induced by TNF

TNF is a potent inducer of inflammation by activating NF-κB. TNF-transgenic (TNFtg) mice develop systemic bone loss and osteoporosis in addition to erosive arthritis by promoting osteoclastogenesis and inhibiting bone formation[40–42]. To further determine whether Wnt4 could directly inhibit inflammation-associated bone loss, we bred TNFtg mice with Wnt4 mice. There was severe paw and joint swelling, often associated with joint deviation in 1-year-old TNFtg mice. μCT and histological analysis revealed that there were extensive joint cartilage destruction and bone erosions due to invasion of inflammatory cells (Supplementary Fig. 3a-e). In contrast, there was significantly less joint swelling, bone erosion and inflammation in TNFtg/Wnt4 mice than in TNFtg mice of comparable age (Supplementary Fig. 3a-e).

Consistent with previous studies, μCT analysis revealed systemic bone loss suffered by 1-year-old TNFtg mice compared with WT mice. However, bone loss in TNFtg/Wnt4 femurs was markedly mitigated (Fig. 3a). Quantitative measurements revealed that, whereas 31% of BMD and 68% of BV/TV were lost in TNFtg mice compared to WT mice, only 18% of BMD and 28% of BV/TV were lost in TNFtg/Wnt4 mice (Fig. 3b). As the reduced bone loss could be due to either increased bone formation or slowed bone resorption or both, we examined the effect of Wnt4 on both components of bone homeostasis. The reduction in the BFR and mineral apposition rate (MAR) in TNFtg mice were alleviated in TNFtg/Wnt4 mice (Fig. 3c). Consistently, histomorphometric analysis also showed 24% greater osteoblast counts in TNFtg/Wnt4 than TNFtg mice (Fig. 3d). Since it has been shown that osteoclastogenesis and bone resorption were enhanced in TNFtg mice, we then examined the effect of Wnt4 on accelerated bone resorption in TNFtg mice. Both histomorphometric analysis and TRAP staining revealed that, while osteoclast activity was higher in TNFtg mice compared to WT controls, it was significantly lower in TNFtg/Wnt4 mice (Fig. 3e,f).

Consistently, the serum concentrations of Ocn were significantly lower in TNFtg mice than that in TNFtg/Wnt4 mice (Fig. 3g). On the other hand, the serum concentrations of Trap5b were significantly higher in TNFtg mice than in TNFtg/Wnt4 mice (Fig. 3h).

We observed that the serum Il-6 concentration in TNFtg/Wnt4 mice was only 55% of that in TNFtg mice (Fig. 3i). Since TNF is a potent activator of NF-κB which is associated with osteoporosis and skeletal aging[16,22,43], Wnt4 might inhibit TNF-induced NF-κB activation in the TNFtg/Wnt4 mice. Immunostaining of active p65 revealed markedly enhanced NF-κB activity in the proximity of trabecular bones in TNFtg mice, while NF-κB staining was significantly reduced in TNFtg/Wnt4 mice (Fig. 3j). Moreover, Wnt4 also inhibited the expression of Cox-2 and Mmp9 in osteoclasts and bone marrow cells induced by TNF *in vivo* (Supplementary Fig. 3f,g).

Wnt4 prevents skeletal aging and bone loss

Aging creates a pro-inflammatory environment with elevated levels of cytokines that contribute to various chronic diseases including osteoporosis or osteopenia[4,44–46]. We further examined whether Wnt4 could protect against natural aging-mediated bone loss or osteopenia. μCT analysis revealed that there was a gradual loss of trabecular bone mass with advancing age from 6 to 24 months in WT mice (Fig. 4a). Further quantitative analysis showed that the most dramatic loss occurred between 6 and 12 months of age and average BMD dropped 42.7% while BV/TV dropped 67.1%. However, the reduction was significantly less with Wnt4 mice, with 32.0% in BMD and 41.9% in BV/TV respectively (Fig. 4b). Histological staining also confirmed that aged Wnt4 mice lost less trabecular bone than aged WT mice (Fig. 4c). Of note, we confirmed that Wnt4 transgene mRNA in bone tissues was still expressed in aged Wnt4 mice using RT-PCR although the levels of Wnt4 mRNA declined over age (Supplementary Fig. 4a,b). Immunostaining also demonstrated that Wnt4 proteins in osteoblasts were strongly detected in aged Wnt4 mice, but weakly in aged WT mice (Supplementary Fig. 4c).

Morphometric measurements for osteoblasts, as well as serum Ocn concentrations, also remained significantly greater in Wnt4 mice than in WT mice across all ages (Fig. 4d,e). Osteoclast number rose in aged 18-month-old WT mice compared to 3-month-old mice (Fig. 4f); however, in aged Wnt4 mice, osteoclast counts became significantly suppressed compared to aged WT mice (Fig. 4f). Notably, while serum Trap5b concentrations were not significantly different between Wnt4 and WT mice at 3 months of age, they increased drastically at 18 or 24 months in WT mice but not in Wnt4 mice (Fig. 4g). Furthermore, serum concentrations of Il-6 also showed a similar trend (Fig. 4h). Finally, we also examined whether natural aging-associated NF-κB activation was suppressed by Wnt4. While immunostaining of active p65 revealed intense NF-κB activities in the vicinity of trabecular bones in aged WT mice, NF-κB activities appeared less prevalent in aged Wnt4 mice (Fig. 4i,j, yellow arrow). Consistently, the expression of Tnf, Cox-2 and Mmp9 was markedly weaker in aged Wnt4 mice compared with aged WT mice (Supplementary Fig. 4d).

Wnt4 inhibits TAK1-NF-κB signaling

Our *in vivo* results suggest that Wnt-4 secreted by osteoblasts may inhibit osteoclast formation and bone resorption in a paracrine fashion. To confirm our hypothesis, we examined whether Wnt4 could directly inhibit osteoclast differentiation using recombinant Wnt4 proteins (rWnt4). As evidenced by TRAP staining, rWnt4 protein significantly inhibited osteoclast differentiation of primary bone marrow macrophages induced by receptor activator of nuclear factor kappa-B (Rankl; Supplementary Fig. 5a). Similarly, the osteoclast-like differentiation of RAW264.7 cells induced by Rankl was also attenuated by Wnt4 (Supplementary Fig. 5b). Real-time RT-PCR confirmed that rWnt4 inhibited the expression of osteoclast marker genes, including *Trap*, *Mmp9* and *Ctsk*, induced by Rankl in bone marrow macrophages and RAW264.7 (Supplementary Fig. 5c,d). Since Wnt4 inhibited the expression of NF-κB target genes *in vivo*, we also examined whether rWnt4 inhibited the expression of NF-κB target genes induced by Rankl. Real-time RT-PCR revealed that rWnt4 potently inhibited induction of NF-κB-dependent genes *Il6* and *Birc3* by Rankl in bone marrow macrophages (Supplementary Fig. 5e) and in RAW264.7 cells (Supplementary Fig. 5f). Consistent with our immunostaining *in vivo*, rWnt4 also significantly suppressed NF-κB-dependent genes *Tnf* and *Cox-2* in bone marrow macrophages (Supplementary Fig. 5g).

To further elucidate the molecular mechanism by which Wnt4 inhibited NF-κB and osteoclastogenesis, we examined each key step of NF-κB activation induced by Rankl. Activation of the Rank receptor leads to association of its cytoplasmic domain with Tnf receptor associated factor 6 (Traf6) which is essential in osteoclast differentiation[47,48]. Traf6 forms a complex with transforming growth factor beta-activated kinase 1 (Tak1) and Tak1-binding protein 2 (Tab2), leading to phosphorylation and activation of Tak1[49]. In canonical NF-κB signaling, Tak1 then phosphorylates IκB kinase (IKK) complex and thereby initiates degradation of Iκbα, followed by phosphorylation and nuclear translocation of p65 to activate downstream target genes[49]. Western blot analysis revealed that rWnt4 potently inhibited the apical step of Tak1 phosphorylation, and the subsequent steps of p65 phosphorylation and the phosphorylation and degradation of Iκbα induced by Rankl (Fig. 5a). Furthermore, rWnt4 also suppressed Rankl-induced nuclear translocation of p65 (Fig. 5b). Moreover, rWnt4 inhibited NF-κB-dependent transcription as determined by the NF-κB-dependent luciferase reporter assay (Fig. 5c).

Since Tak1 also forms a complex with Nemo-like kinase (Nlk) and Tab2 in non-canonical Wnt signaling[27,50], we hypothesized that rWnt4 stimulation may interfere with the formation of the Traf6-Tak1-Tab2 complex induced by Rankl. The co-immunoprecipitation (IP) revealed that Rankl induced the formation of the Traf6-Tak1-Tab2 complex using anti-Traf6 antibodies (Fig. 5d, lane 1 and 2). However, addition of rWnt4 drastically inhibited the formation of the Traf6-Tak1-Tab2 complex (Fig. 5d, **lane 2 and 4**). On the contrary, we observed that rWnt4 stimulation induced the formation of the Tak1-Tab2-Nlk complex, the addition of Rankl partially reduced the formation of the Tak1-Tab2-Nlk complex (Fig. 5d, **lane 3 and 4**). Since Traf6-Tak1 signaling also activates p38 mitogen-activated protein kinase (p38), Jnk and extracellular signal-regulated kinase (Erk), we examined whether rWnt4 inhibited the activation of p38, Jnk and Erk induced by Rankl. Consistently, we found

that rWnt4 proteins also partially inhibited the phosphorylation of Erk, p38 and Jnk induced by Rankl (Supplementary Fig. 5h).

As the nuclear factor of associated T-cells c1 (Nfatc1) is the key transcription factor for osteoclastogenesis[51], we examined the effect of rWnt4 treatment on its expression following Rankl stimulation in bone marrow macrophages. We found that the induction of Nfatc1 by Rankl was repressed by rWnt4 (Fig. 5e). Previously, it has been shown that the activation of NF-κB induced the expression of *Nfatc1*, which in turn activated osteoclast differentiation[52]. Both NF-κB and NFAT consensus binding sites exist at the *Nfatc1* promoter. Upon induction by Rankl, p65 is recruited to the *Nfatc1* promoter to activate its transcription and subsequently the newly-generated Nfatc1 can auto-amplify itself[52]. Chromatin immunoprecipitation (ChIP) assays revealed that rWnt4 significantly suppressed the Rankl-induced p65 binding to the *Nfatc1* promoter (Fig. 5f). Consequently, rWnt4 also potently reduced Nfatc1 binding at its own promoter induced by Rankl (Fig. 5g). While we previously found that Wnt4 activates non-canonical Wnt signaling in MSCs[33], Wnt4 might stimulate canonical Wnt signaling by stabilizing β-catenin. To rule out this possibility, we examined whether rWnt4 proteins increased the levels of cytosolic and nuclear β-catenin in bone marrow macrophages. Subcellular fractionation revealed that, while rWnt3a increased the levels of cytosolic and nuclear β-catenin, rWnt4 did not induce in the accumulation of β-catenin (Fig. 5h). Moreover, we also examined whether rWnt4 induced β-catenin-dependent transcription using a Topflash luciferase reporter. rWnt3a, but not rWnt4, significantly activated the luciferase reporter in bone marrow macrophages (Fig. 5i). In addition, two well-known Wnt/β-catenin target genes, *Axin2* and *Dkk1*, were induced by rWnt3a, but not by rWnt4 (Fig. 5j).

rWnt4 proteins inhibit osteoporosis

To explore the potential clinical utilization of Wnt4, we first tested whether rWnt4 prevented osteoporotic bone loss by inhibiting NF-κB. 3-month-old mice were ovariectomized and intraperitoneally administered with rWnt4 once a day for three weeks. μCT analysis revealed that, while mice that underwent OVX suffered marked loss in trabecular BMD and BV/TV one month after OVX, mice injected with rWnt4 had significantly less bone loss (Supplementary Fig. 6a-c). Histological analysis also confirmed that rWnt4 significantly inhibited trabecular bone loss induced by OVX (Supplementary Fig. 6e–g). Moreover, rWnt4 also reduced serum Trap5b levels (Supplementary Fig. 6h). Immunostaining showed that rWnt4 inhibited NF-κB activity in osteoclasts and adjacent inflammatory cells upon OVX (Supplementary Fig. 6i). Consistently, we found that serum levels of Il-6 and Tnf induced by OVX were significantly reduced by rWnt4 (Supplementary Fig. 6j).

To further evaluate the therapeutic value of rWnt4 proteins, we examined whether rWnt4 could reverse established bone loss in mice induced by OVX. We first performed OVX on 3 month-old mice and waited for one month to establish bone loss. We then administrated the mice with rWnt4 or the vehicle control for one month. μCT analysis revealed that rWnt4 significantly reversed OVX-induced reduction in trabecular BMD and BV/TV (Fig. 6a,b). Histological staining confirmed that rWnt4 reduced trabecular bone loss induced by OVX

(Fig. 6c). Histomorphometric analysis also showed that, while rWnt4 significantly increased osteoblast counts induced by OVX (Fig. 6d), rWnt4 significantly inhibited osteoclast formation (Fig. 6e,f). Consistently, rWnt4 reduced serum Trap5b concentrations induced by OVX (Fig. 6g) whereas it modestly increased serum Ocn concentrations (Fig. 6h). Immunostaining revealed that rWnt4 potently inhibited NF-κB activity in osteoclasts and adjacent bone marrow cells (Fig. 6i), as well as the expression of Tnf, Cox-2 and Mmp9 (Supplementary Fig. 7). rWnt4 also significantly reduced serum concentrations of Il-6 and Tnf induced by OVX (Fig. 6j).

DISCUSSION

Using three different, but complimentary animal models, we demonstrated that Wnt4 could prevent osteoporosis and aging-related bone loss by inhibiting NF-κB, unraveling a novel crosstalk between non-canonical Wnt signaling and NF-κB. The gain- or loss-of-function mutations of Wnt signaling components have been identified in a variety of human bone disorders[26,53,54]. Recently, Wnt5a has been found to enhance osteoclast formation and bone resorption by activating the non-canonical JNK signaling pathway. Wnt5a enhanced osteoclastogenesis induced by Rankl through the Ror2 receptor[32], suggesting that targeting Wnt5a may prevent bone erosion in arthritis. However, Wnt5a-haploinsufficient mice had a bone-loss phenotype with increased adipogenesis in bone marrow[50]. Thus, Wnt5a might not be an ideal therapeutic agent for arthritis and metabolic bone loss. On the contrary, we found that Wnt4 inhibited osteoclastogenesis and bone resorption *in vitro* and *in vivo* by inhibiting NF-κB while promoting bone formation, thereby holding more promising potential as a therapeutic agent for preventing skeletal aging, osteoporosis and arthritis compared to Wnt5a.

Various Wnt ligands can elicit different responses depending on the receptors and cell contexts. Wnt5a acts via Ror2 to enhance the expression of Rank in osteoclast precursors by stimulating the activator protein 1 and promotes Rankl-induced osteoclast formation[32]. Notably, we find that Wnt4 suppresses Tak1 activation induced by Rankl, resulting in the inhibition of IKK/NF-κB activation in macrophages and osteoclast precursors. While Tak1 plays a role in non-canonical Wnt signaling by interacting with Nlk[50], it also modulates canonical Wnt signaling[55,56]. The definitive role of Tak1 in both canonical and non-canonical signaling might depend on cell context and individual Wnt ligands. Based on our results, Wnt4 might activate its receptors to promote Tak1-mediated non-canonical Wnt signaling in osteoclasts, and subsequently sequester Tak1 from effectively binding with Traf6 to induce the NF-κB signaling cascade. Although we showed that Wnt4 promoted Tak1 binding to Nlk, it is possible that Wnt4 might also promote the interaction between Tak1 and the Wnt signaling components, since it has been reported that Ror2 interacts with Tak1[55].

Most drugs currently used for osteoporosis are inhibitors of bone resorption, but cannot restore the significant bone loss that has already occurred at the time of diagnosis. Therefore, a better treatment module for osteoporosis would not only address issues with bone homeostasis, but also control local inflammation[6–8,11]. Multiple Wnt proteins, including Wnt4, have been detected in bone tissues or bone marrow[54,57,58]. Although the

inhibition of aging-associated bone loss and inflammation is mainly based on transgenic overexpression of Wnt4, multiple non-canonical Wnt ligands, including Wnt4, Wnt6, Wnt11 and Wnt16, are expressed in osteoprogenitors[57,58]. They may collectively protect against aging-associated bone loss and inflammation. Importantly, we show that rWnt4 proteins effectively inhibit OVX-induced bone loss by inhibiting NF-κB. While canonical Wnt proteins have potential therapeutic value for treating osteoporosis by promoting bone formation, the constitutive activation of β-catenin might also increase the risk for cancer development which is associated with aging[23,24]. Since Wnt4 does not activate β-catenin in either osteoblasts or osteoclasts, our results suggest that rWnt4 proteins may be a better therapeutic agent for preventing skeletal aging and treating inflammatory bone diseases by inhibiting NF-κB.

ONLINE METHODS

Generation of transgenic mice and experimental animals

We used the plasmid pGL647, which contained the Col2.3 promoter to specifically drive osteoblast-specific gene expression *in vivo*. We subcloned the mouse Wnt4 gene into pGL647, flanked by the Col2.3 promoter. The fragments of the Wnt4 transgene were purified and microinjected into C57BL/6×SJL mouse oocytes (Charles River Laboratory) and the oocytes were surgically transferred to pseudopregnant C57BL/6 dams by the University of Michigan Transgenic Animal Model Core. We screened the founders by PCR using mouse tail genomic DNA and confirmed them by Southern blot analysis. We bred two transgenic founder mice with C57BL/6 mice for six generations to obtain a defined genetic background. TNFtg mice expressing hemizygous human TNF were purchased from Taconic Farms (#1006; B6.Cg(SJL)-Tg(TNF) N21+; Oxnard, California). WT C57BL/6 mice for rWnt4 injection were purchased from Jackson Laboratory (Bar Harbor, Maine). In all experiments, female transgenic mice and female WT littermates as controls were used. We established a sample size of at least 8 mice per group in OVX and aging experiments based on our previous experience[22]. We used a sample size of at least 6 mice per group in TNFtg/Wnt4 experiments. The animals were randomly assigned to procedure groups including sham, OVX and rWnt4 injection. However, not all animal experiments were conducted in a completely blinded fashion. We ovariectomized 3-month-old transgenic and WT mice to induce osteoporosis. Two months after operation, we euthanized the mice and gathered their femurs for histological and μCT analysis. We collected blood samples and isolated serums for serology. Serum ELISA were performed with a mouse Trap5b assay kit (SBA Sciences), an Ocn ELISA kit (Biomedical Technologies), Il-6 and Tnf Quantikine ELISA kits (R&D Systems). All mouse protocols were approved by The University Committee on Use and Care of Animals at the University of Michigan, the Animal Research Committee at the University of California-Los Angeles or both.

Cell culture and viral infection

We grew cells in a humidified 5% CO2 incubator at 37 °C in alpha modified Eagle's medium supplemented with 15% fetal bovine serum (FBS; Invitrogen, California, USA). Viral packaging was prepared as described previously[59]. For viral infection, we plated cells overnight and then infected them with lentiviruses or retroviruses in the presence of

polybrene (6 μg ml^{-1}, Sigma-Aldrich, USA) for 6 h. We then selected the cells with puromycin for 3 days. Resistant clones were pooled and knock-down or over-expression was confirmed via Western blot analysis. For culturing of RAW264.7 cells, we used Dulbecco's modified Eagle's medium supplemented with 10% FBS. For primary bone marrow macrophages, we extracted bone marrow cells from mouse femurs, and treated them with 100 ng ml^{-1} mouse macrophage colony-stimulating factor (M-Csf; R&D systems) for 2 days. This allowed the induction to form osteoclast precursors used in the experiments. For induction of osteoclastogenesis, we treated the osteoclast precursors with 100 ng ml^{-1} mouse Rankl (R&D systems) for up to 3 days. In all *in vitro* experiments involving Wnt3a and Wnt4 recombinant proteins (R&D systems) and Rankl, we used 100 ng ml^{-1}.

Western blot analysis

We lysed cells in RIPA buffer (10 mM Tris-HCL, 1 mM EDTA, 1% sodium dodecyl sulfate [SDS], 1% Nonidet P-40, 1: 100 proteinase inhibitor cocktail, 50 mM β-glycerophosphate, 50 mM sodium fluoride). We then separated lysates on a 10% SDS polyacrylamide gel and transferred to membranes by a semi-dry transfer apparatus (Bio-Rad). We blocked membranes with 5% milk for 1 h and then incubated with primary antibodies overnight. After rinsing, we incubated the immunocomplexes with horseradish peroxidase-conjugated anti-rabbit or anti-mouse IgG (Promega, Madison, WI) and visualized the membranes with SuperSignal Chemiluminiscent substrate (Pierce, Rockford, IL) as previously described[22, 59]. We purchased primary antibodies from the following commercial sources: anti-phospho-Tak1 (1:1000; 4531S; Cell Signaling, Danvers, Massachusetts), anti-Tak1 (1:1000; MAB5307; R&D systems), anti-phospho-p65 (1:2000; 3033S; Cell Signaling), anti-p65 (1:2000; 06-418; Millipore, Billerica, Massachusetts), anti-phospho-Iκbα (1:1000; 9246; Cell Signaling), anti-Iκbα (1:1000; sc-371; Santa Cruz, Santa Cruz, California), anti-phospho-JNK (1:500; 9251; Cell Signaling), anti-JNK (1:1,000; 9258; Cell Signaling), anti-phospho-p38 (1:1000; 9215; Cell Signaling), anti-p38 (1:1000; 8680; Cell Signaling), anti-phospho-Erk (1:1000; 4284; Cell Signaling), anti-Erk (1:1000; 4696; Cell Signaling), anti-Traf6 (2μg for immunoprecipitation; 1:1000 for Western blot; sc-8409; Santa Cruz), anti-Nlk (2μg for immunoprecipitation; AB10206, Millipore), anti-Tab2 (1:1000; 3744; Cell Signaling), anti-Nfatc1 (1:1000; sc-7294; Santa Cruz), anti-HA (1:2000; H9658; Sigma-Aldrich), anti-Tbp (1:2000; T1827; Sigma-Aldrich) and anti-α-tubulin (1:10000; 75168; Sigma-Aldrich).

ALP, ARS and TRAP staining

To induce MSC differentiation, we cultured MSCs in mineralization-inducing media containing 100 μM ascorbic acid, 2 mM β-glycerophosphate and 10 nM dexamethasone. For ALP staining, after induction, we fixed cells with 4% paraformaldehyde and incubated them with a solution of 0.25% naphthol AS-BI phosphate and 0.75% Fast Blue BB dissolved in 0.1 M Tris buffer (pH 9.3). For detecting mineralization, we induced MSCs for 2–3 weeks, fixed the cells with 4% paraformaldehyde and stained them with 2% Alizarin Red solution (Sigma-Aldrich).

To perform TRAP staining and osteoclast quantification, we fixed cells with a mixture of 3% formaldehyde, 67% acetone and 25% citrate solution, and then stained with a TRAP kit

from Sigma Aldrich according to manufacturers' instructions. Images were taken and analyzed using an Olympus IX-51 microscope. We only counted TRAP+ multinucleated cells (>3 nuclei) as osteoclasts.

Luciferase assays

We infected primary bone marrow macrophages with lentiviruses expressing containing NF-κB-dependent or Topflash luciferease reporters (System Biosciences) for 48hrs simultaneously with M-CSF treatment. After stimulation with Rankl or Wnt3a or Wnt4 for 16 h, we isolated cell lysates. We then used a Dual-luciferase® Reporter Assay System to measure luciferase activities as described previously[59].

Real-time RT-PCR and ChIP assays

We isolated total RNA from MSCs using Trizol reagents (Invitrogen). 2 μg aliquots of RNAs were synthesized using random hexamers and reverse transcriptase according to the manufacturer's protocol (Invitrogen). We then performed Real-Time PCR reactions using the QuantiTect SYBR Green PCR kit (Qiagen) and the Icycler iQ Multi-color Real-time PCR Detection System. The primers for 18S rRNA are: forward, 5'-CGGCTACCAC ATCCAAGGAA-3'; reverse, 5'-GCTGGAATTACCGCGGCT-3'. The primers for *Runx2* are: forward, 5'-AGGGACTATGGCGTCAAACA-3'; reverse, 5'-GGCTCACGTCGCTCACTT-3'. The primers for Sp7 are: forward, 5'-CGCTTTGTGCCTTTGAAAT-3'; reverse, 5'- CCGTCAACGACGTTATGC-3'. The primers for *Bglap* are: forward, 5'-AGCAAAGGTGCAGCCTTTGT-3'; reverse, 5'-GCGCCTGGGTCTCTTCACT-3'. The primers for *Alp* are: forward, 5'-GGACAGGACACACACACACA-3'; reverse, 5'- CAAACAGGAGAGCCACTTCA-3'. The primers for *Ibsp* are: forward, 5'- ACAATCCGTGCCACTCACT-3'; reverse, 5'-TTTCATCGAGAAAGCACAGG -3'. The primers for *Trap* are: forward, 5'-GTGCTGCTGGGCCTACAAAT -3'; reverse, 5'- TTCTGGCGATCTCTTTGGCAT-3'. The primers for *MMP9* are: forward, 5'- TCCTTGCAATGTGGATGT -3'; reverse, 5'-CTTCCAGTACCAACCGTCCT-3'. The primers for *Ctsk* are: forward, 5'-GAAGAAGACTCACCAGAAGCAG -3'; reverse, 5'- TCCAGGTTATGGGCAGAGATT -3'. The primers for *Birc3* are: forward, 5'-ACGCAGCAATCGTGCATTTTG-3'; reverse, 5'- CCTATAACGAGGTCACTGACGG -3'. The primers for *Cox2* are: forward, 5'-AACCCAGGGGATCGAGTGT -3'; reverse, 5'- CGCAGCTCAGTGTTTGGG -3'. The primers for *Tnf* are: forward, 5'-CTGTAGCCCACGTCGTAGC-3'; reverse, 5'-TTGAGATCCATGCCGTTG-3'. The primers for *Dkk1* are: forward, 5'-CTCATCAATTCCAACGCGATCA-3'; reverse, 5'-GCCCTCATAGAGAACTCCCG-3'. The primers for *Axin2* are: forward, 5'-TGACTCTCCTTCCAGATCCCA-3'; reverse, 5'-TGCCCACACTAGGCTGACA-3'. The primers for *Wnt4* (endogenous) are: forward, 5'-CTGGAGAAGTGTGGCTGTGA-3'; reverse, 5'-CAGCCTCGTTGTTGTGAAGA -3'. The primers for *Opg* are: forward, 5'-ACCCAGAAACTGGTCATCAGC-3'; reverse, 5'-CTGCAATACACACACTCATCACT-3'. The primers for *Tnfsf11* are: forward, 5'-CAGCTATGATGGAAGGCTCA-3'; reverse, 5'-GACTTTATGGAACCCGA-3'.

For extraction of tissue RNA, we dissected mouse femurs and pulverized them in liquid nitrogen. After extracting total RNA as described above, we removed residual genomic

DNA using Turbo DNA-free DNase removal kit (Ambion). For RT-PCR, primers for transgene specific Wnt4 are: forward, 5'-CTAAAGCCATTGACGGCTGC-3'; reverse, 5'-GCGTAATCTGGAACATCATATGGG-3'. Primers for β-actin are: forward, 5'-CGTCTTCCCCTCCATCG -3'; reverse, 5'-CTCGTTAATGTCACGCAC-3'.

We performed ChIP assays using a ChIP assay kit (Upstate, USA) following the manufacturer's recommendation. Briefly, we incubated cells with a dimethyl 3,3' dithiobispropionimidate-HCl (Pierce) solution (5 mM) for 10 min at room temperature, followed by formaldehyde treatment for 15 min in a 37 °C water-bath. For each ChIP reaction, we used 2×10^6 cells. We then quantified resulting precipitated DNA samples with Real-time PCR, and expressed data as the percentage of input DNA. Antibodies for ChIP assays were purchased from the following commercial sources: polyclonal anti-p65 (Millipore); polyclonal anti-NFATc1 (Santa Cruz). The primers for *Nfatc1* are: forward, 5'-CTGTGTTCCCACATGTCCTC-3'; reverse, 5'- GCGACTGCAGTGTGTTCTTT-3'. 9kb downstream for *Nfatc1* are: forward, 5'- CTGGCACCAAAGTTGAGAGA-3'; reverse, 5'-GATGGCTCTACCTGCACAGA -3'.

OVX, bone histomorphometry, and scoring of arthritic joint swelling

We performed OVX or sham operation on 3-month-old female WT and Wnt4 mice under isofluorane anesthesia. For the preventive model, rWnt4 proteins (8 μg kg^{-1}) were intraperitoneally injected daily for three weeks immediately after the surgery. For dual-labeling, mice received intraperitoneal injection of calcein (0.5 mg per mouse, Sigma-Aldrich) ten and three days before euthanasia. Mice were euthanized one month after OVX. For the therapeutic model, we first performed OVX on 3 month-old mice and waited for one month to establish bone loss. Mice received intraperitoneal injection of rWnt4 (20 μg kg^{-1}) or vehicle control daily for one month before collection of bone samples. Eight to twelve mice were used in each group.

Following euthanasia, we fixed right femurs in 70% ethanol for 48 h and embedded in methyl methacrylate. 8 μm longitudinal sections were either stained with Toluidine blue for osteoblast count or examined under fluorescent microscope to evaluate BFR and MAR as described previously[22]. We fixed left femurs in 10% formaldehyde and embedded them in paraffin for preparation in 5 μm-thick sections. We analyzed osteoclast parameters after TRAP staining as described. For all bright-field and fluorescent microscopy analysis, we used Olympus-IX51 inverted microscope with SPOT advanced 4.0 and CellSens software.

We scored the swelling of hindpaws on 1-year-old TNFtg and TNFtg/Wnt4 mice on a scale of 0 to 3, as previously described[60,61]: 1 = mild arthritis (mild swelling of joint and paw); 2 = moderate arthritis (severe swelling and joint deviation); 3 = severe arthritis (ankylosis detected upon flexion). We used histological sections of hindpaw and ankle joints to examine the tibiotalar and interdigital joints, and performed μCT imaging to further evaluate bone erosion and destruction of joint space associated with arthritis.

Immunostaining and μCT analysis of mice

We extracted femurs from euthanized mice and fixed them in 10% neutral buffered formalin for 24 hrs. For μCT scanning, the specimens were fitted in a cylindrical sample holder (20.5 mm in diameter) with the long axis of the femur perpendicular to the X-ray source. We used a Scanco μCT40 scanner (Scanco Medical) set to 55 kVp and 70 μA. The bone volume (mm^3) over tissue volume and bone mineral density in the region of interest were measured directly with μCT Evaluation Program V4.4A (Scanco Medical). We defined the regions of interest as the areas between 0.3 mm and 0.6 mm proximal to the growth plate in the distal femurs, in order to include the secondary trabecular spongiosa. We used a threshold of 250 was used for evaluation of all scans[22]. For visualization, we imported the segmented data and reconstructed them as a 3D-image displayed in μCT Ray V3.0 (Scanco Medical).

After scanning, we decalcified the specimens, sectioned them for staining as previously described[22]. Antibodies used include rabbit polyclonal anti-NLS-p65 (600-401-271; 1:200; Rockland), rabbit polyclonal anti-Mmp9 (38898; 1:500; Abcam), rabbit polyclonal anti-Tnf (34674, 1:200; Abcam), and rabbit polyclonal anti-Cox2 (15191, 1:400, Abcam). For quantification of p65 positive staining, we selected at least 10 images from each section per femur, measured the integral optical density (IOD) of nuclear-stained p65 using the Image Pro Plus 6.0 software (MediaCybernetics). We normalized the IOD by stained area, and presented the data as reported previously[62].

Statistical analysis

Numerical data and histograms were expressed as the mean ± standard deviation. Two tailed Student's t-test was performed between two groups and a difference was considered statistically significant with $P < 0.05$.

Supplementary Material

Refer to Web version on PubMed Central for supplementary material.

ACKNOWLEDGEMENTS

We thank Dr. John Adams for valuable advices. This work was supported by US National Institute of Dental and Craniofacial Research Grants and National Institute of Arthritis and Musculoskeletal and Skin Diseases.

REFERENCES

1. Manolagas SC, Jilka RL. Bone marrow, cytokines, and bone remodeling. Emerging insights into the pathophysiology of osteoporosis. N. Engl. J. Med. 1995; 332:305–311. [PubMed: 7816067]
2. Zaidi M. Skeletal remodeling in health and disease. Nat. Med. 2007; 13:791–801. [PubMed: 17618270]
3. Manolagas SC, Parfitt AM. What old means to bone. Trends Endocrinol Metab. 2010; 21:369–374. [PubMed: 20223679]
4. Chien KR, Karsenty G. Longevity and lineages: toward the integrative biology of degenerative diseases in heart, muscle, and bone. Cell. 2005; 120:533–544. [PubMed: 15734685]
5. Bruunsgaard H, et al. Predicting death from tumour necrosis factor-alpha and interleukin-6 in 80-year-old people. Clin Exp Immunol. 2003; 132:24–31. [PubMed: 12653832]

6. Weitzmann MN, Pacifici R. Estrogen deficiency and bone loss: an inflammatory tale. J Clin. Inv. 2006; 116:1186–1194.
7. McClean R. Proinflammatory cytokines and osteoporosis. Curr Osteoporos Rep. 2009; 7:134–139. [PubMed: 19968917]
8. Lopez-Otin C, Blasco MA, Partridge L, Serrano M, Kroemer G. The hallmarks of aging. Cell. 2013; 153:1194–1217. [PubMed: 23746838]
9. Teitelbaum SL. Bone resorption by osteoclasts. Science. 2000; 289:1504–1508. [PubMed: 10968780]
10. Wagner EF, Karsenty G. Genetic control of skeletal development. Curr. Opin. Genet. Dev. 2001; 11:527–532. [PubMed: 11532394]
11. Raisz LG. Pathogenesis of osteoporosis: concepts, conflicts, and prospects. J Clin. Inv. 2005; 115:3318–3325.
12. Riggs BL, Khosla S, Melton LJ III. A unitary model for involutional osteoporosis: estrogen deficiency causes both type I and type II osteoporosis in postmenopausal women and contributes to bone loss in aging men. J Bone Miner. Res. 1998; 13:763–773. [PubMed: 9610739]
13. Khosla S, Riggs BL. Pathophysiology of age-related bone loss and osteoporosis. Endocrinol. Metab. Clin. North Am. 2005; 34:1015–1030. [PubMed: 16310636]
14. Sun L, et al. FSH directly regulates bone mass. Cell. 2006; 125:247–260. [PubMed: 16630814]
15. Ghosh S, Karin M. Missing pieces in the NF-κB puzzle. Cell. 2002; 109(Suppl.):S81–S96. [PubMed: 11983155]
16. Boyce BF, Yao Z, Xing L. Functions of nuclear factor kappaB in bone. Ann. N Y Acad. Sci. 2010; 1192:367–375. [PubMed: 20392262]
17. Jimi E, Ghosh S. Role of nuclear factor-κB in the immune system and bone. Immunol. Rev. 2005; 208:80–87. [PubMed: 16313342]
18. Krum SA, Chang J, Miranda-Carboni G, Wang CY. Novel functions for NF-κB: inhibition of bone formation. Nat. Rev. Rheumatol. 2010; 6:607–611. [PubMed: 20703218]
19. Almeida M, Han L, Ambrogini E, Bartell SM, Manolagas SC. Oxidative stress stimulates apoptosis and activates NF-kappaB in osteoblastic cells via a PKCbeta/p66shc signaling cascade: counter regulation by estrogens or androgens. Mol. Endocrinol. 2010; 24:2030–2037. [PubMed: 20685851]
20. Jimi E, et al. Selective inhibition of NF-κB blocks osteoclastogenesis and prevents inflammatory bone destruction in vivo. Nat. Med. 2004; 10:617–624. [PubMed: 15156202]
21. Chen Q, et al. DNA damage drives accelerated bone aging via an NF-κB-dependent mechanism. J Bone Miner. Res. 2013; 5:1214–1228. [PubMed: 23281008]
22. Chang J, et al. Inhibition of osteoblastic bone formation by nuclear factor-kappaB. Nat Med. 2009; 15:682–689. [PubMed: 19448637]
23. Anastas JN, Moon RT. WNT signalling pathways as therapeutic targets in cancer. Nat Rev Cancer. 2013; 13:11–26. [PubMed: 23258168]
24. MacDonald BT, Tamai K, He X. Wnt/β-catenin signaling: components, mechanisms, and diseases. Dev. Cell. 2009; 17:9–26. [PubMed: 19619488]
25. Regard JB, Zhong Z, Williams BO, Yang Y. Wnt signaling in bone development and disease: making stronger bone with Wnts. Cold Spring Harb Perspect Biol. 2012; 4:1–12.
26. Baron R, Kneissel M. WNT signaling in bone homeostasis and disease: from human mutations to treatments. Nat Med. 2013; 19:179–192. [PubMed: 23389618]
27. Veeman MT, Axelrod JD, Moon RT. A second canon. Functions and mechanisms of beta-catenin-independent Wnt signaling. Dev. Cell. 2003; 5:367–377. [PubMed: 12967557]
28. Seifert JR, Mlodzik M. Frizzled/PCP signalling: a conserved mechanism regulating cell polarity and directed motility. Nat Rev Genet. 2007; 8:126–138. [PubMed: 17230199]
29. McNeill H, Woodgett JR. When pathways collide: collaboration and connivance among signalling proteins in development. Nat Rev Mol Cell Biol. 2010; 11:404–413. [PubMed: 20461097]
30. Lako M, et al. Isolation, characterisation and embryonic expression of WNT11, a gene which maps to 11q13.5 and has possible roles in the development of skeleton, kidney and lung. Gene. 1998; 219:101–110. [PubMed: 9757009]

31. Qiu W, Chen L, Kassem M. Activation of non-canonical Wnt/JNK pathway by Wnt3a is associated with differentiation fate determination of human bone marrow stromal (mesenchymal) stem cells. Biochem Biophys Res Commun. 2011; 413:98–104. [PubMed: 21875572]
32. Maeda K, et al. Wnt5a-Ror2 signaling between osteoblast-lineage cells and osteoclast precursors enhances osteoclastogenesis. Nat. Med. 2012; 18:405–412. [PubMed: 22344299]
33. Chang J, et al. Noncanonical Wnt-4 signaling enhances bone regeneration of mesenchymal stem cells in craniofacial defects through activation of p38 MAPK. J Biol. Chem. 2007; 282:30938–30948. [PubMed: 17720811]
34. Krebsbach PH, et al. Transgenic expression of COL1A1-chloramphenicol acetyltransferase fusion genes in bone: differential utilization of promoter elements in vivo and in cultured cells. Mol. Cell. Biol. 1993; 13:5168–5174. [PubMed: 8355676]
35. Liu F, et al. Expression and activity of osteoblast-targeted Cre recombinase transgenes in murine skeletal tissues. Int J Dev Biol. 2004; 48:645–653. [PubMed: 15470637]
36. Khosla S, Westendorf JJ, Oursler MJ. Building bone to reverse osteoporosis and repair fractures. J Clin. Inv. 2008; 118:421–428.
37. Halleen JM, et al. Tartrate-resistant acid phosphatase 5b: a novel serum marker of bone resorption. J Bone Miner. Res. 2000; 15:1337–1345. [PubMed: 10893682]
38. Pacifici R, et al. Effect of surgical menopause and estrogen replacement on cytokine release from human blood mononuclear cells. Proc Natl Acad Sci USA. 1991; 88:5134–5138. [PubMed: 2052592]
39. Jilka RL, et al. Increased osteoclast development after estrogen loss: mediation by interleukin-6. Science. 1992; 257:88–91. [PubMed: 1621100]
40. Hayward MD, et al. An extensive phenotypic characterization of the hTNFα transgenic mice. BMC Physiology. 2007; 7:13. [PubMed: 18070349]
41. Guo R, et al. Ubiquitin ligase Smurf1 mediates tumor necrosis factor-induced systemic bone loss by promoting proteasomal degradation of bone morphogenetic signaling proteins. J Biol. Chem. 2008; 283:23084–23092. [PubMed: 18567580]
42. Yao Z, Xing L, Boyce BF. NF-kappaB p100 limits TNF-induced bone resorption in mice by a TRAF3-dependent mechanism. J Clin. Inv. 2009; 119:3024–3034.
43. Lam J, et al. TNF-alpha induces osteoclastogenesis by direct stimulation of macrophages exposed to permissive levels of RANK ligand. J Clin Invest. 2000; 106:1481–1488. [PubMed: 11120755]
44. Pandey AC, et al. MicroRNA profiling reveals age-dependent differential expression of nuclear factor κB and mitogen-activated protein kinase in adipose and bone marrow-derived human mesenchymal stem cells. Stem Cell Res. Ther. 2011; 2:49. [PubMed: 22169120]
45. Garnero P, Sornay-Rendu E, Chapuy MC, Delmas PD. Increased bone turnover in late postmenopausal women is a major determinant of osteoporosis. J Bone Miner Res. 1996; 11:337–349. [PubMed: 8852944]
46. Ginaldi L, Di Benedetto MC, De Martinis M. Osteoporosis, inflammation and ageing. Immun Ageing. 2005; 2:14. [PubMed: 16271143]
47. Lomaga MA, et al. TRAF6 deficiency results in osteopetrosisa and defective interleukin-1, CD40, and LPS signaling. Genes Dev. 1999; 13:1015–1024. [PubMed: 10215628]
48. Bai S, Zha J, Zhao H, Ross FP, Teitelbaum SL. Tumor necrosis factor receptor-associated factor 6 is an intranuclear transcriptional coactivator in osteoclasts. J Biol Chem. 2008; 283:30861–30867. [PubMed: 18768464]
49. Mizukami J, et al. Receptor activator of NF-kappaB ligand (RANKL) activates TAK1 mitogen-activated protein kinase kinase kinase through a signaling complex containing RANK, TAB2, and TRAF6. Mol. Cell. Biol. 2002; 22:992–1000. [PubMed: 11809792]
50. Takada I, et al. A histone lysine methyltransferase activated by non-canonical Wnt signalling suppresses PPAR-gamma transactivation. Nat. Cell Biol. 2007; 9:1273–1285. [PubMed: 17952062]
51. Teitelbaum SL, Ross FP. Genetic regulation of osteoclast development and function. Nat. Rev. Genet. 2003; 4:638–649. [PubMed: 12897775]
52. Asagiri M, et al. Autoamplification of NFATc1 expression determines its essential role in bone homeostasis. J Exp. Med. 2005; 202:1261–1269. [PubMed: 16275763]

53. Holmen SL, et al. Essential role of β-catenin in postnatal bone acquisition. J. Biol. Chem. 2005; 280:21162–21168. [PubMed: 15802266]

54. Lories RJ, Corr M, Lane NE. To Wnt or not to Wnt: the bone and joint health dilemma. Nat. Rev. Rheumatol. 2013; 9:328–339. [PubMed: 23459013]

55. Winkel A, et al. Wnt-ligand-dependent interaction of TAK1 (TGF-beta-activated kinase-1) with the receptor tyrosine kinase Ror2 modulates canonical Wnt-signalling. Cell Signal. 2008; 20:2134–2144. [PubMed: 18762249]

56. Li M, et al. TAB2 scaffolds TAK1 and NLK in repressing canonical Wnt signaling. J Biol. Chem. 2010; 285:13397–13404. [PubMed: 20194509]

57. Sugimura R, et al. Noncanonical Wnt signaling maintains hematopoietic stem cells in the niche. Cell. 2012; 150:351–365. [PubMed: 22817897]

58. Heinonen KM, Vanegas JR, Lew D, Krosl J, Perreault C. Wnt4 enhances murine hematopoietic progenitor cell expansion through a planar cell polarity-like pathway. PLoS One. 2011; 6:e19279. [PubMed: 21541287]

59. Fan Z, et al. BCOR regulates mesenchymal stem cell function by epigenetic mechanisms. Nat. Cell Biol. 2009; 11:1002–1009. [PubMed: 19578371]

60. Redlich K, et al. Osteoclasts are essential for TNF-alpha-mediated joint destruction. J Clin. Inv. 2002; 110:1419–1427.

61. Thwin MM, et al. Effect of phospholipase A2 inhibitory peptide on inflammatory arthritis in a TNF transgenic mouse model: a time-course ultrastructural study. Arthritis Res Ther. 2004; 6:282–294. [PubMed: 15535841]

62. Li J, et al. LATS2 suppresses oncogenic Wnt signaling by disrupting β-catenin/BCL9 interaction. Cell Rep. 2013; 5:1650–1663. [PubMed: 24360964]

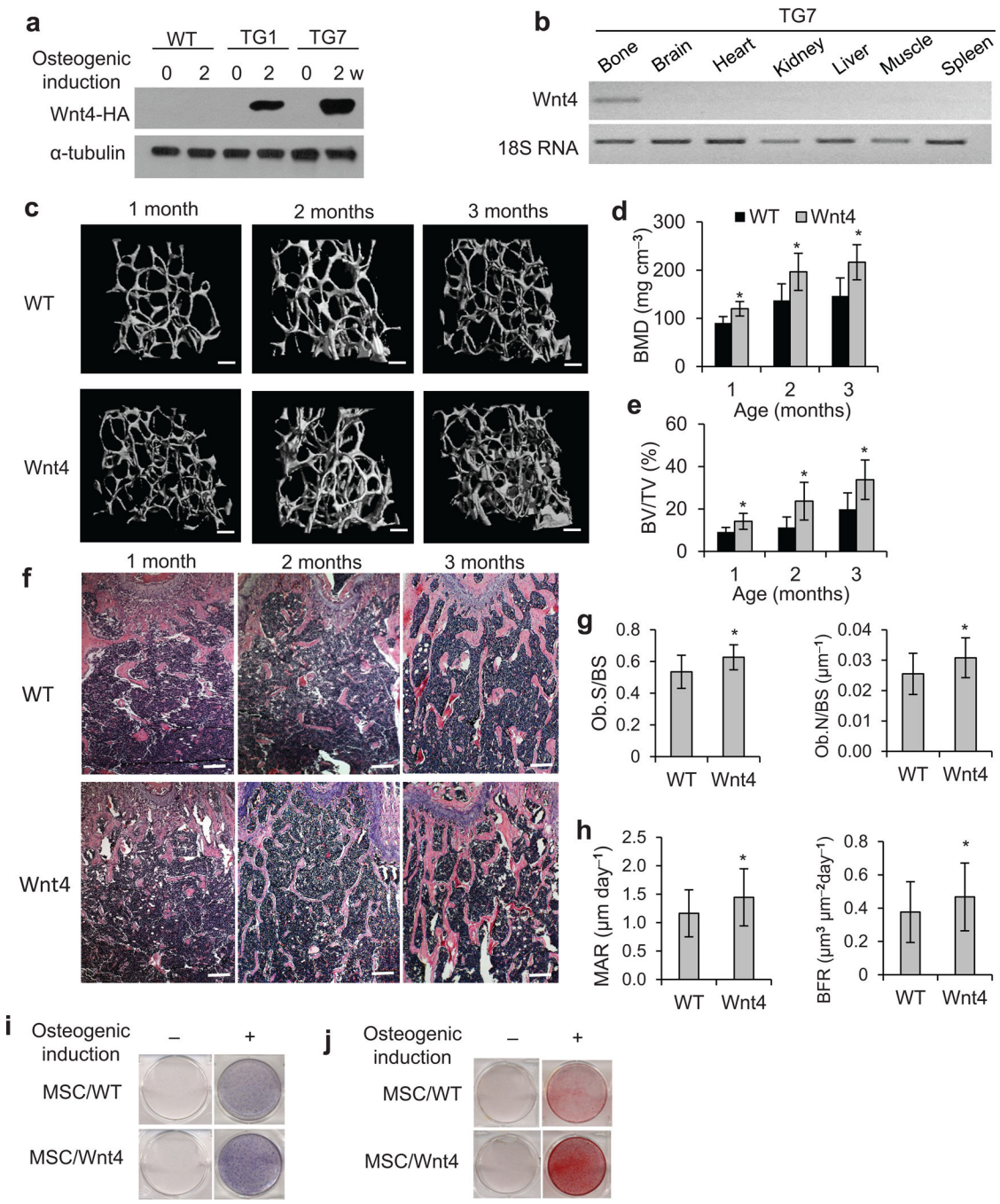

Figure 1.

Wnt4 promotes postnatal bone formation *in vivo*. (**a**) Western blot showing Wnt4 expression in primary calvarial cells extracted from WT and Wnt4 mice following osteogenic induction. (**b**) RT-PCR analysis of *Wnt4* mRNA expression in various tissues and organs. (**c–e**) μCT reconstruction (**c**), BMD (**d**) as well as BV/TV (**e**) of metaphysis regions of distal femurs from 1, 2, and 3-month-old WT and Wnt4 mice. Scale bars, 200 μm; *n* = 12 per group. (**f**) H&E staining of femur sections from 1, 2, and 3-month-old WT (*n* = 8 per group) and Wnt4 mice (*n* = 10 per group). Scale bars, 300 μm. Ob.S, osteoblast surface. Ob.N, osteoblast

number. BS, bone surface. (**g**) Histomorphometric analysis of osteoblast counts in 3-month-old Wnt4 ($n = 10$) vs WT mice ($n = 8$). (**h**) BFR and MAR measurements from dual-fluorescent calcein labeling of 3-month-old Wnt4 ($n = 10$) vs WT mice ($n = 8$). (**i**) ALP staining of femur bone marrow MSCs from Wnt4 vs WT mice, after osteogenic induction. (**j**) ARS of MSCs from Wnt4 vs WT mice after osteogenic induction. * $P < 0.05$, unpaired two-tailed t-test.

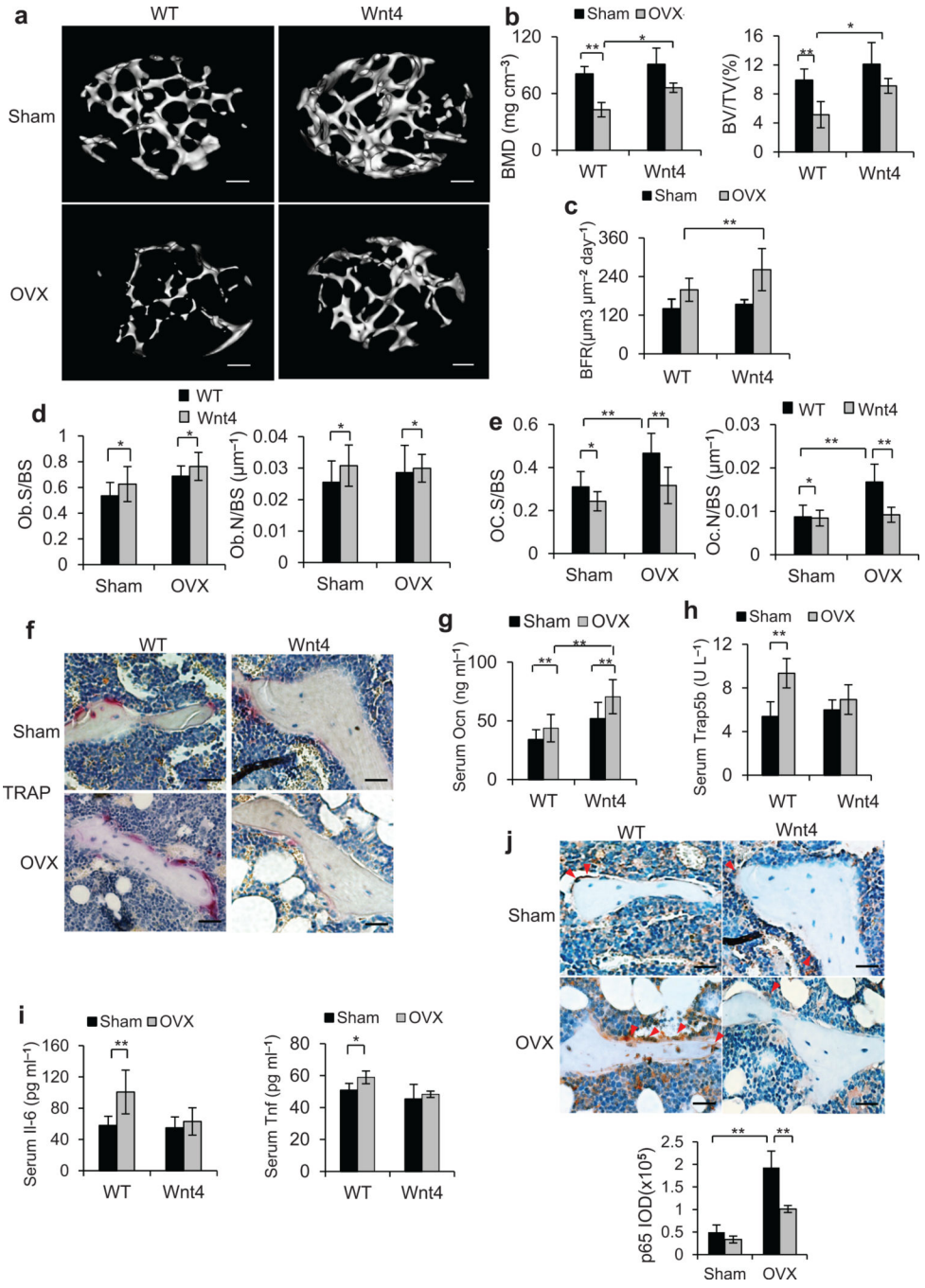

Figure 2.

Wnt4 attenuates osteoporosis induced by OVX. (**a,b**) μCT reconstruction (**a**) of metaphysis of distal femurs, as well as BMD and BV/TV (**b**) in WT vs Wnt4 mice at two months post OVX. Scale bars, 200 μm. (**c**) BFR measurement of calcein dual labeling in WT vs Wnt4 mice two months after OVX or sham operation. (**d, e**) Morphometric analysis of osteoblast counts (**d**) and osteoclast counts (**e**) in WT vs Wnt4 mice after OVX or sham operation. (**f**) TRAP staining of femur sections from WT and Wnt4 mice after OVX or sham operation. (**g–i**) ELISA of serum concentrations of Ocn (**g**), Trap5b (**h**), Il-6 and Tnf (**i**) in WT vs Wnt4

mice after OVX or sham operation. Scale bars, 30μm. (**j**) Immunostaining and quantification of active p65 in trabecular bone cells and surrounding bone marrow cells in WT and Wnt4 mice after OVX or sham operation. Scale bars, 30 μm. IOD, integral optical density. For **b–e**, and **g–j**, $n = 8$ for sham groups; $n = 12$ for OVX groups. *$P < 0.05$, ** $P < 0.01$, unpaired two-tailed t-test.

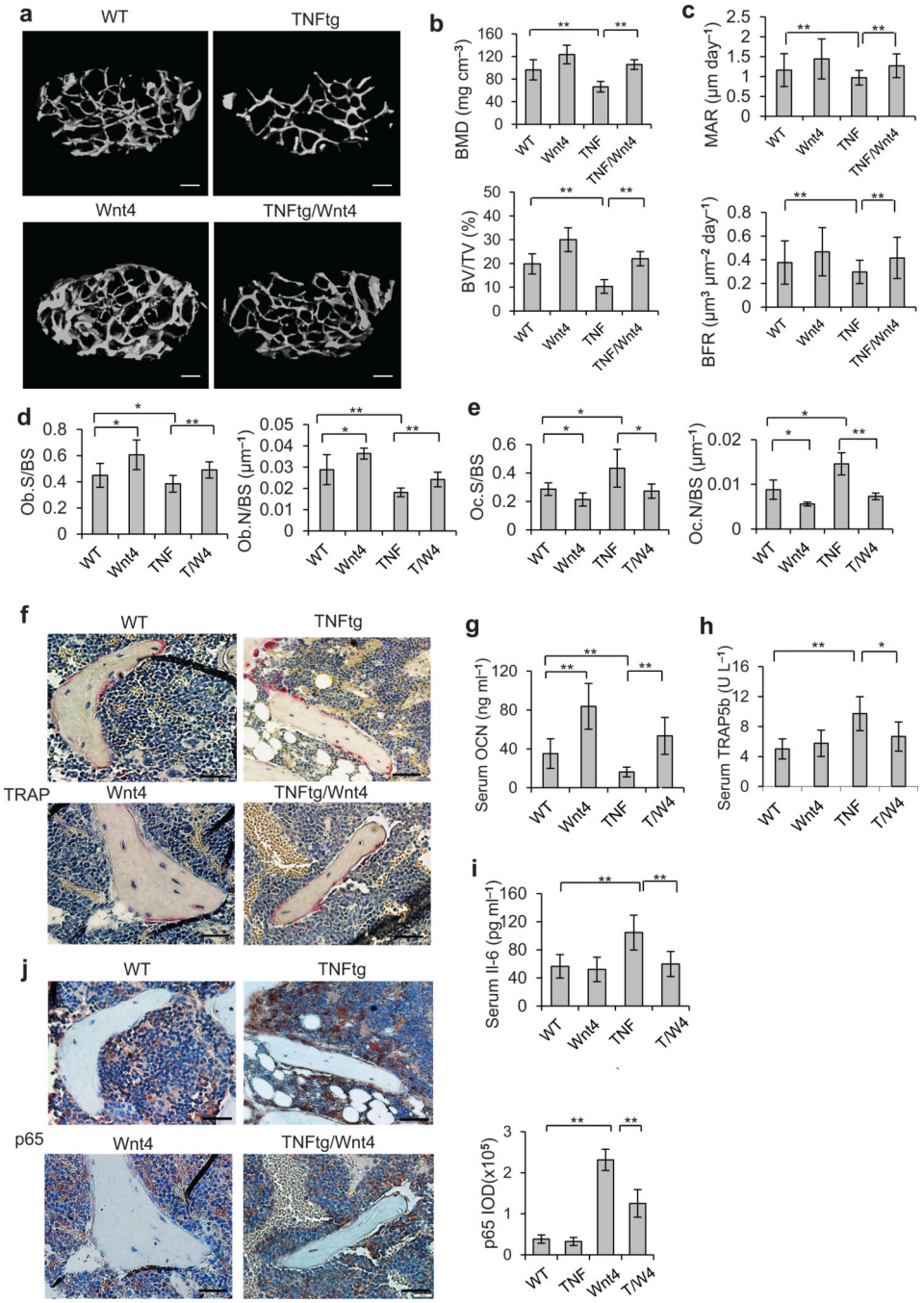

Figure 3.

Wnt4 inhibits TNF-induced bone loss and NF-κB activation. (**a,b**) μCT reconstruction (**a**), BMD and BV/TV (**b**) of distal femoral metaphysis regions from WT, Wnt4, TNFtg and TNFtg/Wnt4 mice. Scale bars, 200 μm. (**c**) Comparisons of MAR and BFR in TNFtg mice and TNFtg/Wnt4 mice. (**d,e**) Morphometric analysis of osteoblast counts (**d**) and osteoclast counts (**e**) in TNFtg mice and TNFtg/Wnt4 mice. (**f**) TRAP staining of osteoclasts surrounding trabecular bones in WT, Wnt4, TNFtg and TNFtg/Wnt4 mice. Scale bars, 40 μm. (**g–i**) ELISA of Ocn (**g**), Trap5b (**h**) and Il-6 (**i**) concentrations in serum collected from

WT, Wnt4, TNFtg and TNFtg/Wnt4 mice. (**j**) Immunostaining with anti-active p65 and quantification of NF-κB activity surrounding the trabecular bone in WT, Wnt4, TNFtg and TNFtg/Wnt4 mice. Scale bars, 40μm. TNF, TNFtg mice; T/W4, TNFtg/Wnt4 mice. For **b–e**, and **g–j**, $n = 6$ per group for WT and WNT4 mice; $n = 8$ per group for TNFtg and TNFtg/Wnt mice. *$P < 0.05$, ** $P < 0.01$, unpaired two-tailed t-test.

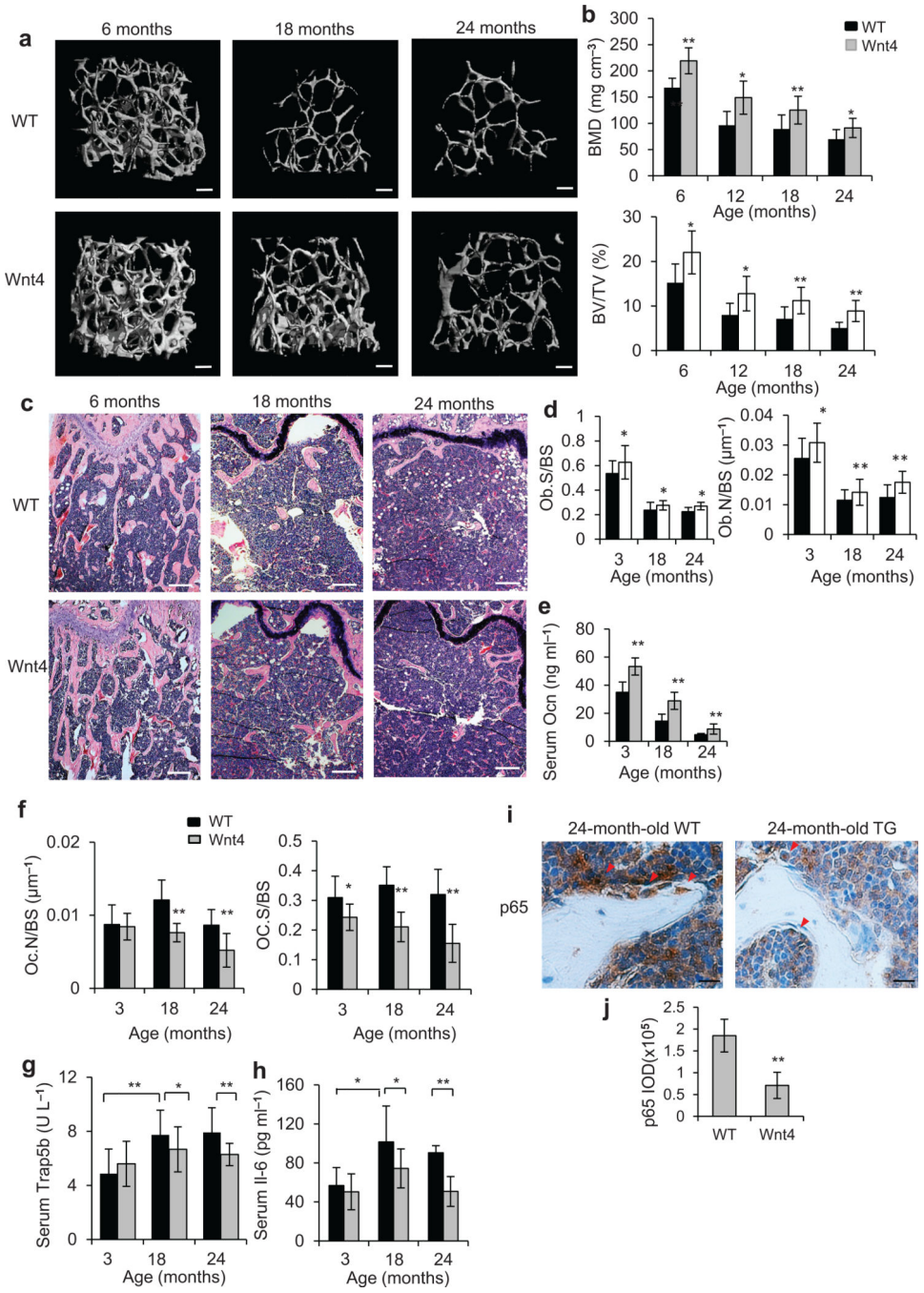

Figure 4.

Wnt4 attenuates skeletal aging by inhibiting NF-κB. (**a–c**) μCT reconstruction (**a**), BMD and BV/TV (**b**), as well as H&E staining (**c**) of distal femoral metaphysis regions from 6-, 18- and 24-months-old WT and Wnt4 mice. Scale bars, 200 μm (**a**); 300 μm (**c**). (**d**) Morphometric analysis of osteoblast counts in distal femoral metaphysis from 3-, 18- and 24-months-old WT and Wnt4 mice. (**e**) ELISA of Ocn concentrations in serum from 3-, 18- and 24-months-old WT and Wnt4 mice. (**f**) Morphometric analysis of osteoclast counts in distal femoral metaphysis from 3-, 18- and 24-months-old WT and Wnt4 mice. (**g,h**) ELISA

of Trap5b (**g**) and Il-6 (**h**) concentrations in serum from 3-, 18- and 24-months-old WT and Wnt4 mice. (**i**) Immunostaining with anti-active p65 and quantification of NF-κB activity surrounding the trabecular bones from 24-months-old WT and Wnt4 mice. Scale bars, 25 μm. For **b**, and **d–i**, $n = 12$ mice per group. *$P < 0.05$, ** $P < 0.01$, unpaired two-tailed t-test.

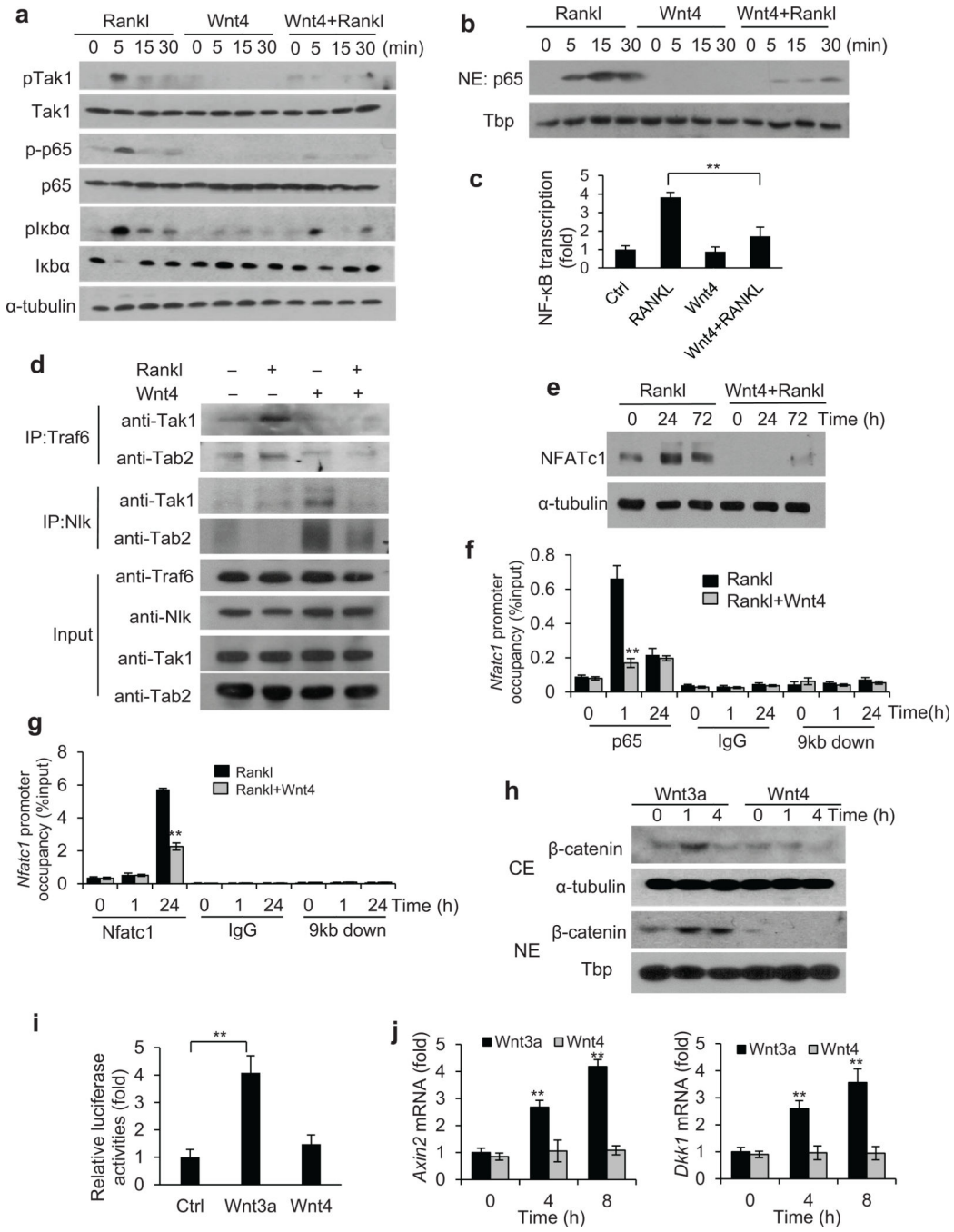

Figure 5.

Wnt4 inhibits NF-κB by interfering with TAK1-TRAF6 binding. (**a**) Immunoblots showing the phosphorylation of Tak1, p65 and Iκbα in bone marrow macrophages after treatment of Rankl, rWnt4 and rWnt4 with Rankl. (**b**) Immunoblots showing p65 and Tata-binding protein (Tbp) in nuclear extracts of bone marrow macrophages treated with Rankl, rWnt4 and rWnt4 with Rankl. (**c**) Relative NF-κB-dependent luciferase reporter activities in bone marrow macrophages after treatment of Rankl, rWnt4 and rWnt4 with Rankl. (**d**) Immunoblots showing the Traf6-Tak1-Tab2 complex formation induced by Rankl in bone

marrow macrophages. (**e**) Immunoblots showing the induction of Nfatc1 in bone marrow macrophages after treatment of Rankl, and rWnt4 with Rankl. (**f**) ChIP assays of the recruitment of p65 to the *Nfatc1* promoter induced by Rankl. Anti-IgG and primers designed at 9 kb downstream of transcription start site (TSS) were used as negative control. (**g**) ChIP assays of Nfatc1 binding to the *Nfatc1* promoter. (**h**) Immunoblots of β-catenin in cytosolic extract (CE) and nuclear extract (NE) of bone marrow macrophages treated with Wnt3a and Wnt4. (**i**) Relative Topflash luciferase activities in bone marrow macrophages treated with Wnt3a or Wnt4. (**j**) Real-time RT-PCR of *Axin2* and *Dkk1* in bone marrow macrophages treated with Wnt3a or Wnt4. $n = 3$; * $P < 0.05$; ** $P < 0.01$; unpaired two-tailed t-test.

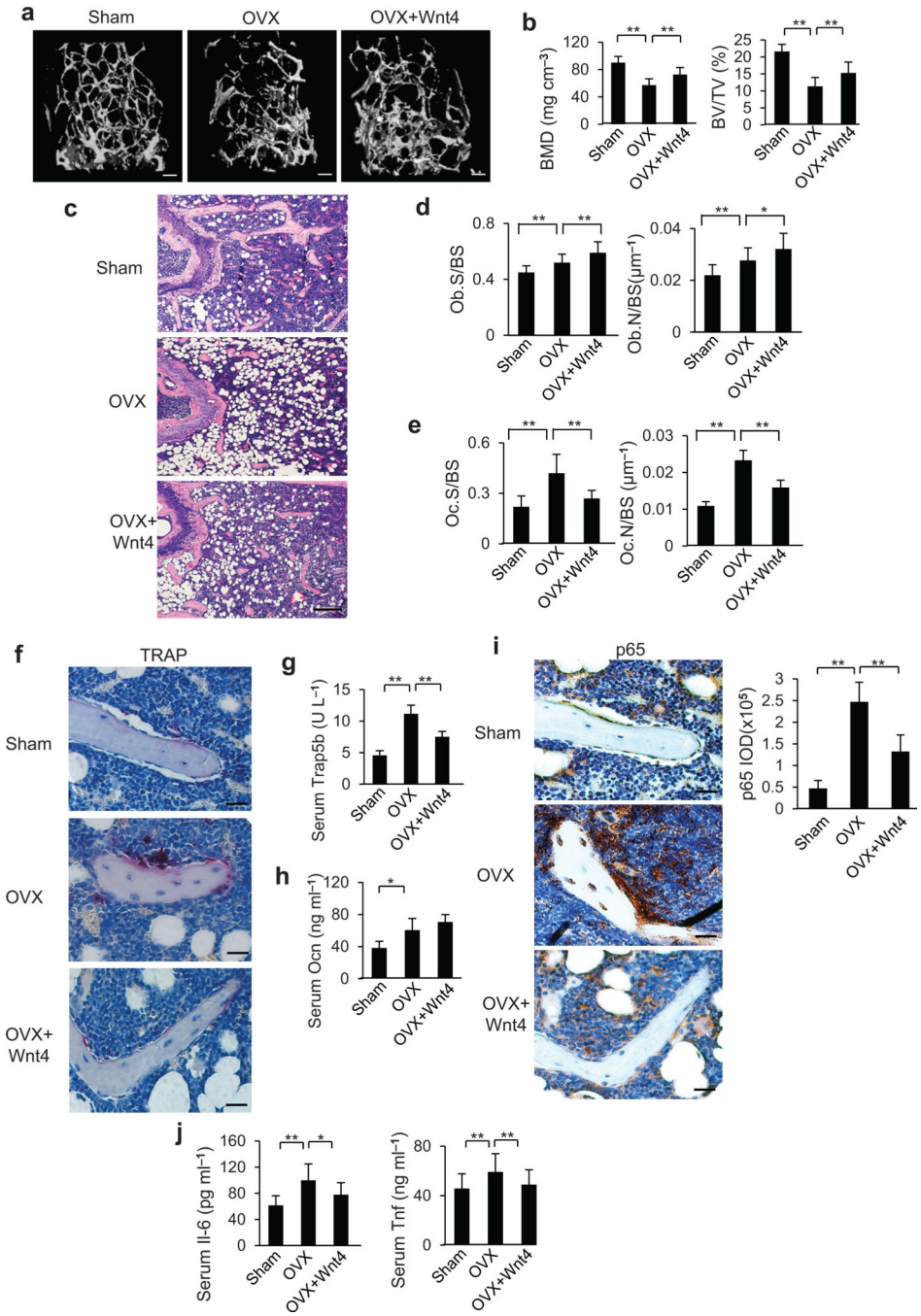

Figure 6.

rWnt4 proteins attenuates established bone loss by inhibiting NF-κB. (**a–c**) μCT reconstruction (**a**), BMD and BV/TV (**b**), as well as H&E staining (**c**) of distal femoral metaphysis regions from mice after sham operation, OVX and OVX with rWnt4 injection. Scale bars, 200 μm (**a**); 300 μm (**c**). (**d,e**) Morphometric analysis of osteoblast (**d**) and osteoclast (**e**) counts in distal femoral metaphysis from mice after sham operation, OVX and OVX with rWnt4 injection. (**f**) TRAP staining showing osteoclasts surrounding trabecular bones in mice after sham operation, OVX and OVX with rWnt4 injection. Scale bars, 30μm.

(**g,h**) ELISA of Trap5b (**g**) and Ocn (**h**) concentrations in serum from mice after sham operation, OVX and OVX with rWnt4 injection. (**i**) Immunostaining with anti-active p65 and quantification of NF-κB activity surrounding the trabecular bones from mice after sham operation, OVX and OVX with rWnt4 injection. Scale bars, 30 μm. (**j**) ELISA of Il-6 and Tnf concentrations in serum from mice after sham operation, OVX and OVX with rWnt4 injection. $n = 8$ mice for sham group; $n = 12$ mice per group for mice receiving OVX and OVX with rWnt4 injection. *$P < 0.05$, ** $P < 0.01$, unpaired two-tailed t-test.